Optimal shape of a cold-neutron triple-axis spectrometer

K. Lefmann [a,b,*], U. Filges [c], F. Treue [a], J.J.K. Kirkensgård [d,e], B. Plesner [d], K.S. Hansen [d,f], K.H. Klenø [a,b]

[a] Nanoscience and eScience Centers, Niels Bohr Institute, University of Copenhagen, Universitetsparken 5, 2100 Copenhagen Ø, Denmark
[b] European Spallation Source, University of Lund, St. Algatan 4, Lund, Sweden
[c] Laboratory for Development and Methods, Paul Scherrer Institute, 5232 Villigen PSI, Switzerland
[d] Institute of Nature and Models, Roskilde University, Denmark
[e] Department of Basic Sciences and Environment, Faculty of Life Sciences, University of Copenhagen, Denmark
[f] Mid-Greenland High School, Nuuk, Greenland

ARTICLE INFO

ABSTRACT

We have performed a McStas optimization of the primary spectrometer for a generic 40 m long, cold-neutron triple-axis spectrometer with a doubly focusing monochromator. The optimal design contains an elliptically focusing guide, a virtual source point before a low-grade PG monochromator, and non-equidistant focusing at the monochromator. The flux at 5 meV shows a gain factor 12 over the "classical" design with a straight $12 \times 3 \, cm^2$, $m=2$ guide and a vertically focusing PG monochromator. In addition, the energy resolution was found to be improved. This unexpectedly large design improvement agrees with the Liouville theorem and can be understood as the product of many smaller gain factors, combined with a more optimal utilization of the beam divergence within the guide. Our results may be relevant for a possible upgrade of a number of cold-neutron triple-axis spectrometers—and for a possible triple-axis spectrometer at the European Spallation Source.

© 2010 Elsevier B.V. All rights reserved.

1. Introduction

The triple-axis spectrometer (TAS) is one of the oldest and most well-known types of neutron instrumentation; designed by the Nobel Laureate B.N. Brockhouse already in the 1950s [1]. Later ingenious instrument development has improved on the original design, most importantly the cold neutron moderator [2], and the neutron guide, which allows the transport of cold neutrons ($\lambda > 2 \, A$) far away from the background-rich region around the neutron source [3]. An excellent recent textbook has been devoted to the description and use of the TAS [4]. However, there may still be some room for design improvements, which is the topic we investigate in this article.

Many cold-neutron TAS exist at continuous neutron sources around the world. Most of these instruments have adopted the 1990s design, where the neutrons are transported by a 30–50 m curved supermirror guide, and reflected down to the sample by a vertically focusing monochromator made by mosaic pyrolytic graphite (PG). Some examples of TAS of this design are IN-12 and IN-14 at ILL [5], TASP and RITA-2 at PSI [6], FLEX at HZB [7], and SPINS at NIST [8]. New developments in guide technology and the appearance of doubly focusing monochromators, implemented

e.g. at PANDA (FRM-2) [9] and MACS (NIST) [10] have spawned ideas of upgrade of a number of cold-neutron TAS, e.g. at ILL, PSI, and HZB.

In this article, we will address the question of how to improve the configuration of the primary spectrometer of the cold-neutron TAS. We have simulated different instrument designs by use of the Monte Carlo ray-tracing package McStas [11]. We start by investigating the characteristics of the classical TAS design and then perform a number of controlled design changes. The optimal design is then found by a "free" computer optimization of all parameters, which is again restricted to find a realizable design. Finally, we explain the found results in terms of phase space densities and the Liouville theorem and discuss the optimal design of the complete cold neutron triple-axis spectrometer.

2. Design and simulation

The baseline design for these simulations is defined in terms of moderator, guide, and monochromator and can be seen as an idealization of the RITA-2 spectrometer at PSI. The moderator has a uniform neutron distribution over its $15 \times 10 \, cm^2$ area and follows a typical cold spectrum with an intensity corresponding to a medium flux source. We have chosen the parameters valid at 2002 for SINQ running at 1 mA current, as already used in Ref. [12]. The guide is 40 m long with $m=2$ supermirrors and a reflectivity of 90.5% at $q = mQ_c$ ($\alpha = 4.38$ in McStas units) and has

* Corresponding author at: Nanoscience and eScience Centers, Niels Bohr Institute, University of Copenhagen, Universitetsparken 5, 2100 Copenhagen Ø, Denmark. Tel.: +45 35320476.
E-mail address: lefmann@fys.ku.dk (K. Lefmann).

a cross-section of $30 \times 120 \, mm^2$. The guide starts 1.5 m from the moderator with a 5 m straight section, followed by a 20 m curved section with a curvature of $R=2$ km, and finally a 15 m straight section. The monochromator is placed 0.5 m after the guide opening and is made from PG with 30′ mosaicity and a reflectivity of 80%. The monochromator has five vertically focusing blades, each 30 mm tall and 200 mm wide, with a 1 mm gap between blades. The sample is positioned 1.5 m from the monochromator, the smallest distance achievable in practice due to shielding and sample environment requirements.

All simulations were performed with 5×10^7 neutron rays (2×10^7 when only flux numbers were required), corresponding to 5 min (2 min) processing time on a standard 2 GHz laptop for the straight guide. In most simulations, the monochromator was set to reflect neutrons of 5.0 meV ($\lambda = 4.045 \, Å$). We recorded neutrons reaching the sample area, which is $1 \times 1 \, cm^2$. The absolute flux value was for the baseline design found to $\Psi = 4.03(2) \times 10^6 \, n/s/cm^2$, with a spread (FWHM) of the incoming neutron energy of $\Delta E_i = 127 \, \mu eV$. These baseline results were used as the starting point for the optimization procedure, see Table 1.

Simulation of a very similar primary spectrometer has been performed for the RITA-2 spectrometer at PSI, and the results for both flux and (in particular) energy resolution of vanadium scans were found to agree well with the performance of the real spectrometer over a wide wavelength range [12,13]. This serves as a validation of the results of the present simulations, both in terms of absolute flux value and (in particular) on relative flux improvements and energy resolution. The energy spread of the incoming neutrons should be viewed in relation to the acceptance of the secondary spectrometer. For example, at RITA-2 this value is 141 μeV without collimation. The energy resolution of the complete spectrometer is found (for incoherent scattering) by adding the two contributions in quadrature.

2.1. Controlled design upgrades

Our initial simulations contained a series of individual optimizations to the design. The optimizations were performed in the order given below, and were mostly performed by optimizing the sample flux while varying a single parameter at a time. The gains mentioned should be understood as *additional* gain compared to last design change. The corresponding results are listed in Table 1.

- Improving the supermirror coating. This resulted in a surprisingly small flux increase (5%), reached at $m=4$.

Table 1
Results of the optimizations: flux (Ψ) and energy spread (ΔE_i) at the sample position.

Change	Ψ ($10^6 \, n/s/cm^2$)	ΔE_i (μeV)
Baseline	4.03(2)	127
Guide coating $m=4$	4.26(3)	130
Guide width 5 cm	6.62(5)	195
Guide height 16 cm	8.38(7)	195
Mosaicity 70′	12.24(8)	183
Doubly focusing mono.	13.52(8)	153
Fine-tuning mono.	15.82(6)	172
Elliptical guide, focus on mono.	26.7(4)	165
Virtual source, fine-tuning	35.7(3)	237
Free optimization	79.6(4)	137
Restrained, free optimization	44.9(2)	85

The individual steps are described closer in the text.

- Increasing the guide width. This gave a large flux gain of almost 60% for $w=5$ cm, but a broadening in energy of around 40%.
- Increasing the guide height and inserting additional blades in the monochromator. This gave a further flux increase of 25% for $h=16$ cm.
- Increasing the PG mosaicity. A flux gain of almost 50% was found for $\eta = 70′$, surprisingly without change in ΔE
- Doubly focusing monochromator, composed of $25 \times 25 \, mm^2$ tiles. This resulted in an additional flux gain of 10% and an improvement of energy spread to almost the baseline design.
- Increasing the guide-monochromator distance to 2.4 m and the PG mosaicity to 45′. This gain was small, around 15%, and there was a small increase of energy spread.

Increasing the monochromator-sample distance to 2.1 m to almost obtain equidistant (Rowland) focusing decreased the energy spread by 30%, but simultaneously lowered the flux by 40%. Hence, this idea was abandoned.

At the end of this simulation round, we received a flux gain of a factor 3.9 and an enlarged spread of the incoming energy of only 35%. This agrees rather well with earlier optimization studies for RITA-2 [14].

2.2. Optimization with an elliptical guide

The simulations in the previous section were performed with a conventional guide system with a constant cross-section. Recent developments in guide technology has enabled the construction of fully elliptical guides with strongly improved focusing possibilities [15]. Thus, it was natural to include elliptical guides in our design.

For truly elliptical guides, there is the complication that line-of-sight between moderator and monochromator will increase the fast-neutron background. At present a number of suggestion to circumvent this problem exist, none of which will cause substantial flux loss, including a bending of the elliptical guide, placing a beam stop within the guide, and accepting the (limited) additional background from the fast neutrons [16–18]. It is, however, at present not clear which of these solutions will prove most efficient in practice. Therefore, we here continue the optimization using only neutron flux and energy spread as optimization parameters, ignoring the line-of-sight complication.

We have continued the optimization, replacing the curved guide with an elliptical guide of the same dimensions. As a reassurance, we first reproduced the results below for a guide of infinite focal length. Next, we used focal lengths of 2.0 m—meaning that both the focal points were placed 2.0 m outside the guide. This provided a significant flux gain (65%) over the straight guide. Then, we created a virtual source by using 1.4 m focal length and placing the monochromator at 2.9 m to obtain Rowland focusing. This was accompanied by fine tuning of the monochromator parameters, and additional height to the monochromator. This scheme gave a flux gain of additional 35%, but again an increase in the energy spread. In total, this design gives us a 9-fold increase in flux at the cost of a factor 2 increase in energy spread.

2.3. Total computer optimization

Having obtained the encouraging results by the manual single-parameter optimizations, we went to explore unknown territory by performing a total computer optimization of most parameters describing the guide-monochromator system. The total number of parameters was 14, small enough to be achievable by the Simplex algorithm already implemented in McStas.

To avoid the degradation of the energy spread, seen is the hand-optimizations above, we entered the energy spread into a Figure-of-Merit given by

$$\text{FoM} = \Psi^2/\Delta E_i. \qquad (1)$$

This was implemented into McStas by writing a Figure-of-Merit monitor component, and using its output as the parameter to be maximized by the Simplex algorithm.

The results of the free computer optimization are presented in Table 1. It can be seen that these optimizations gave an additional flux gain of more than a factor 2, resulting in a total gain factor of 20; with almost the same energy spread as the baseline instrument. However, by inspecting the solution this was found to feature a very large guide ($180 \times 120 \text{ mm}^2$ at both start and exit) and a 400 mm tall monochromator, 4.7 m from the guide exit. This was deemed unreasonable, since the fast-neutron background would be much too high and the vertical divergence would exceed $7°$.

In the second attempt, we restricted the guide size indirectly by placing a slit, limiting the virtual source point to $80 \times 50 \text{ cm}^2$, while limiting the monochromator height to 300 mm. From this arrangement, the optimal figuration was found to have a sample flux 25% better than the manually optimized solution, while the energy spread was surprisingly 35% lower than that of the baseline design.

Studying the optimal parameters, we can see that the final instrument has a number of interesting features. Foremost, the distance between guide opening and the 60′ PG monochromator is increased to 4.05 m, while the virtual source point is placed already after 0.60 m. The corresponding beam profiles are shown in Figs. 1 and 2. Since the monochromator-sample distance is still fixed to 1.5 m, the monochromator focusing does not fulfill the Rowland condition. Hence, to optimize the energy resolution, the monochromator support was turned $17°$ away from the half scattering angle, while keeping the blades in the correct scattering angle. This scheme is known *e.g.* from the non-equidistant monochromatic focusing analyzer mode at RITA-2 [19,20].

3. Phase space considerations

The large gain in both neutrons flux and energy resolution found by the computerized optimizations calls for a closer investigation of the final design. Our guideline to obtain insight
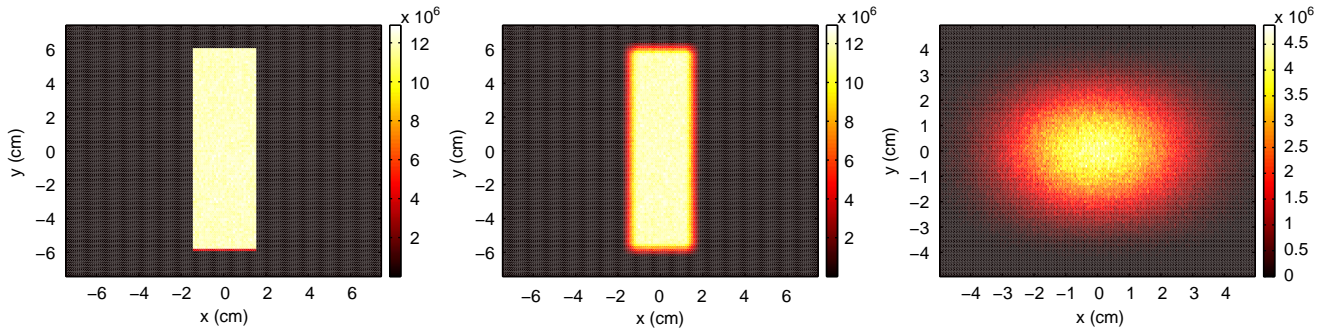

Fig. 1. Simulated beam cross-sections for 5 meV neutrons at different positions in the baseline instrument, given in flux units: n/(s cm²). (a) At the exit of the straight/curved guide; (b) 0.20 m before the monochromator; (c) at the sample position.

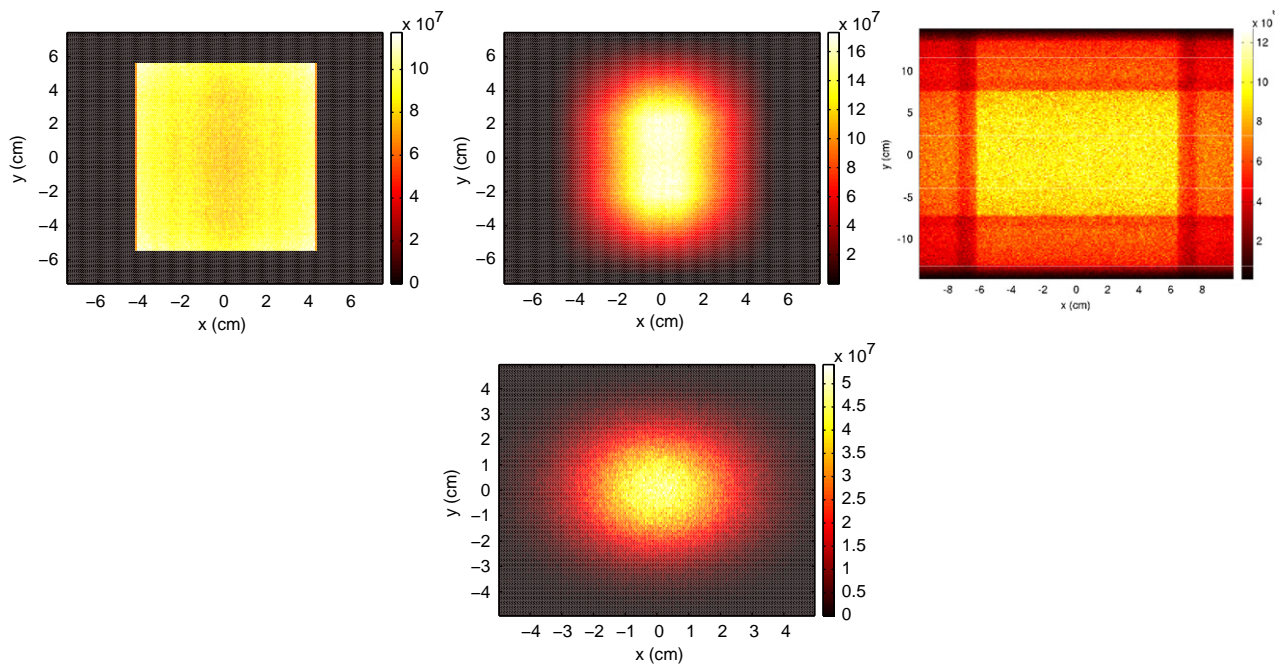**Fig. 2.** Simulated beam cross-sections for 5 meV neutrons at different positions in the final instrument, given in flux units: n/(s cm²). (a) At the exit of the elliptical guide; (b) at the virtual source point 0.60 m after the guide end; (c) 0.20 m before the monochromator; (d) at the sample position.

Table 2
Brilliance simulated at different positions along the spectrometer, given in 10^6 brilliance units, as found by integrating over flux in a 1% wavelength band within ± 30 arc minutes divergence angle.

Position	Baseline design	Elliptical, manual	Elliptical, optimized
Moderator	1.43(1)	1.50(1)	1.53(2)
Guide entry	1.50(1)	1.50(1)	1.54(2)
Guide exit	1.42(1)	1.34(1)	1.31(2)
Before mono.	1.41(1)	1.33(1)	1.23(2)
After mono.	0.54(1)	0.63(1)	0.79(1)
At sample	0.51(1)	0.69(1)	0.79(1)

Results are given for the baseline design TAS, for the manually optimized spectrometer with an elliptical guide, and finally for the fully (computer) optimized solution.

in the functioning of the guide-monochromator system is the Liouville theorem [21], stating that the phase space density of a particle ensemble cannot increase under elastic processes.

The true statistic-mechanical phase space contains six variables: the particle position, $\mathbf{r}$, and velocity, $\mathbf{v}$. Since all neutrons travel along the same direction, we essentially integrate out the position along the beam direction by counting the number of neutrons passing an area during a time much longer than the typical time between the arrival of two neutrons. We are thus left with five variables: two spatial, two concerning divergence, and the magnitude of the neutron velocity (or equivalently the wavelength). The phase space density is now given by the neutron flux per unit of divergence per wavelength interval. This strongly resembles the definition of brilliance used in X-ray instrumentation, where the unit is typically photons/(s mm^2 mrad^2 0.1% wavelength bandwidth) [22]. In our investigation below, we will use the brilliance unit neutrons/(s cm^2 deg^2 1% wavelength bandwidth).

To calculate the neutron brilliance in a ray-tracing simulation, we tracked the neutron flux through a small area (1 cm^2), for neutrons within a particular divergence interval (± 10 arc minutes or ± 30 arc minutes in both directions), when the moderator is limited to emit a narrow wavelength band ($\delta\lambda/\lambda = 1\%$). The simulated neutron flux for the wider divergence thus equals the brilliance units defined above. We sampled the brilliance at several places along the beam path:

- At the moderator surface.
- At the guide entry.
- At the guide exit.
- Just before the monochromator.
- Just after the monochromator.
- At the sample position.

The brilliance was calculated for both the original TAS (the baseline design), for the manually optimized spectrometer, and for the fully optimized TAS. The results are listed in Table 2. We see that the baseline design loses almost $\frac{2}{3}$ of its brilliance at the monochromator, while the hand optimized elliptical design loses a factor $\frac{1}{2}$, and the elliptical design only loses 45%. This is, however, not enough to account for the factor 12 in flux gain with a concurrent decrease in energy spread.

4. Discussion

Our results show that the classical design of a primary spectrometer for a cold-neutron TAS can be strongly improved. The new design includes an elliptical guide, focusing on a virtual source point. Placed 3.4 m after this virtual source, a doubly focusing monochromator performs non-equidistant focusing onto the sample position.

In our simulations, the sample flux is found to increase by a factor 12, while the energy spread decreases. The phase-space density analysis shows that the brilliance at the sample position is improved. The flux can be written as the brilliance multiplied with the energy spread and the divergence range, in the case where energy and divergence are uncorrelated (this will be shown below). This implies that the performance of the new design can be understood by a combination of a better transport (factor 1.6) of the brilliance onto the sample with lower energy spread (factor 0.65), and a higher divergence (factor 10) transported onto the sample position. This is verified by the divergence simulations, shown in Figs. 3–5.

In the final solution, the value of the brilliance at the sample is about 50% of that at the moderator. Taking Liouvilles theorem into account, there may thus be up to a factor 2 to gain for future design optimizations. However, when taking into account that the used reflectivity of PG (80%) is probably the highest diffraction reflectivity of any material, the maximal remaining gain factor is 1.5. One of the ways forward could be to employ anisotropic mosaicity of the PG material to minimize the increase in vertical divergence introduced by the mosaicity. It should also be considered to use non-elliptical guide shapes, which may produce an even better focusing at the virtual source point [23].

In cases where high divergence is unwanted, *e.g.* for single crystal diffraction, or when the design is used for a powder diffractometer, a simple Soller collimator can be employed. Additional simulations have showed that for tight collimations (20′), the new design is a factor 3 better than the baseline design, most of which (a factor 2) comes from the increase in vertical divergence. The energy resolution of the final solution is still about 20% better than the baseline design with collimation.

To understand the improvement in energy spread over the manually optimized solution, we consider the correlation between the horizontal divergence and wavelength, shown in Fig. 6. It can be seen that the shape of the divergence-wavelength "ellipsoid" has been rotated by the use of the non-equidistant focusing, so that the divergence and energy are essentially uncorrelated, since all divergences essentially represent the same energy. This insight allows for designing a controlled tuning of the resolution ellipsoid by rotating the analyzer mount to be somewhere between the Rowland position and the present optimal position. Much of the power of the TAS during the decades was based upon the fact that the resolution function can be shaped to fit the particular problem, *e.g.* by varying incident wavelength, collimations, and scattering angles [4]. Here we show that we can shape the correlations between energy and divergence.

The full four-dimensional (q,ω) resolution function can, however, only be investigated by studying a design of the complete spectrometer. It can be foreseen that the secondary spectrometer for a fully optimized TAS will be a multi-analyzer design, either of the RITA-type with closely spaced analyzers [24,25], a multi-analyzer system with broad coverage like MACS at NIST [10] or the ILL flat-cone type [26], or of the even more advanced multi-energy CAMEA type [27]. It is, however, too early to discuss the performance of these combinations of possible primary and secondary spectrometers. Additional simulations elucidating this problem are underways [28].

In the light of the current work towards realizing the European Spallation Source (ESS) [29], it is worth considering whether the spectrometer designed in this work would be suitable for a long-pulsed spallation source. Here, one could utilize the full time-integrated neutron flux produced at the moderator—the best estimate is that this will equal the ILL flux, giving an impressive sample flux of 9×10^8 neutrons/(s cm^2) at 5 meV. An important benefit of this design is that fast-neutron background can be
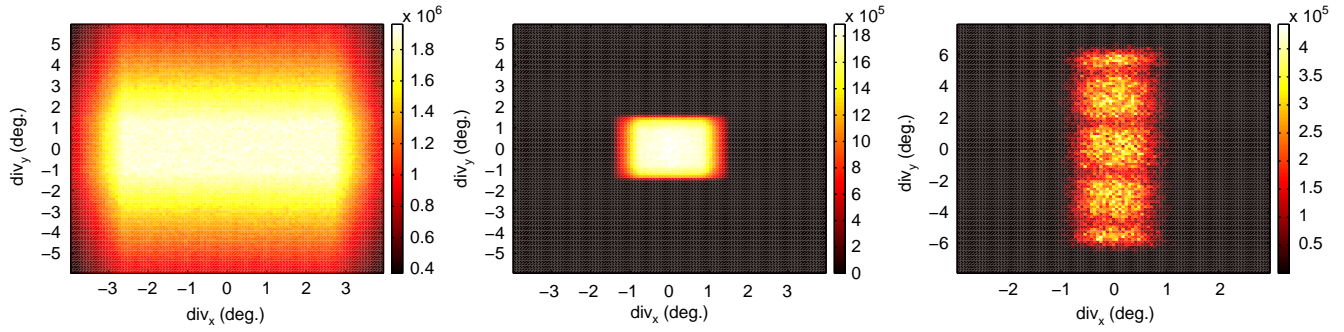
Fig. 3. Divergence plots sampled at a $10 \times 10\,\text{mm}^2$ area at the baseline instrument using the full wavelength band of $\Delta\lambda = 2\,\text{Å}$. The data are presented in units of wavelength-integrated brilliance: $n/(s\,\text{cm}^2\,\text{deg}^2)$. (a) The guide entry; (b) the guide exit; (c) the sample position.
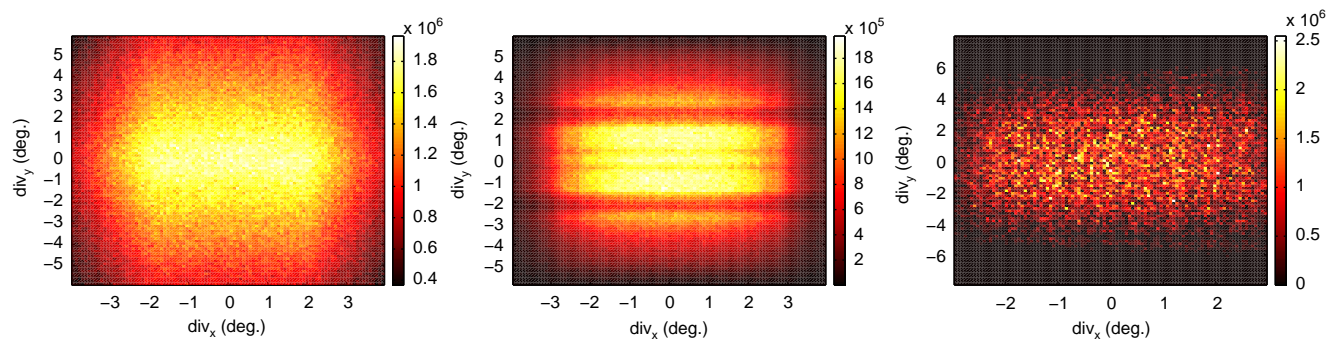

Fig. 4. Divergence plots sampled at a $10 \times 10\,\text{mm}^2$ area at the hand optimized elliptical instrument using the full wavelength band of $\Delta\lambda = 2\,\text{Å}$. The data are presented in units of wavelength-integrated brilliance: $n/(s\,\text{cm}^2\,\text{deg}^2)$. (a) The guide entry; (b) the guide exit; (c) the sample position.
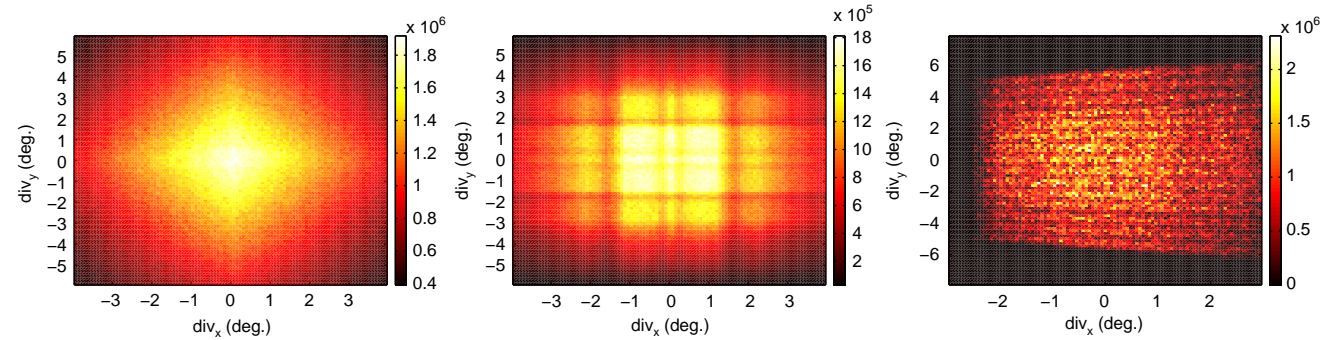

Fig. 5. Divergence plots sampled at a $10 \times 10\,\text{mm}^2$ area at the final instrument using the full wavelength band of $\Delta\lambda = 2\,\text{Å}$. The data are presented in units of wavelength-integrated brilliance: $n/(s\,\text{cm}^2\,\text{deg}^2)$. (a) The guide entry; (b) the guide exit; (c) the sample position.
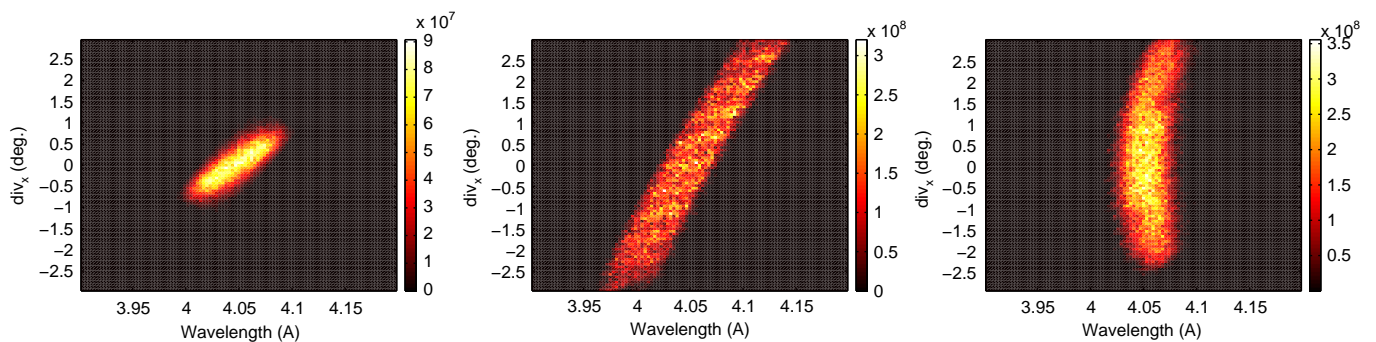

Fig. 6. Correlations between wavelength and horizontal divergence at the sample position, in arbitrary units. (a) The baseline design; (b) the manually optimized solution; (c) the final elliptical solution.

strongly suppressed by time-of-flight analysis, in particular when using incoming wavelengths which have frame overlap with fast neutrons from the previous pulse. For a 40 m instrument, this would imply that the incoming wavelengths should stay below 6 Å, which in practice is almost always the case for a cold-neutron TAS. As an additional advantage, thermal-neutron background and second-order scattering from the monochromator could here easily be suppressed by a slow chopper.

5. Conclusion

Based upon extensive simulations, we suggest a design of a primary spectrometer for a triple-axis spectrometer, consisting of an elliptical guide, a virtual source point, and a doubly focusing monochromator, which uses non-equidistant focusing. The performance of this primary spectrometer is strongly superior to the classical design, with a gain in incoming flux by a factor 12, with a slight improvement in energy resolution. Future detailed analysis, including background estimates, will show whether it will be worth building such an instrument on an existing or future neutron source. In particular, the issue of line-of-sight between moderator and monochromator should be considered. In addition, it will be interesting to study this type of design for a primary spectrometer for a thermal neutron instrument; and for use on a long-pulse spallation source like ESS.

The phase-space analyses shows that our suggested primary spectrometer for a TAS—or other similar instruments—does not yet have the optimal shape and that it theoretically should be possible to improve it by a factor 1.5.

As a final remark, we like to add that a very similar solution to the TAS optimization problem has recently been found by an independent work [30]. This work differs from ours in that they consider an addition of an elliptical guide to an existing conventional guide. However, the design of virtual source and doubly focusing monochromators are very similar. The agreement between the solutions is remarkable, not least due to the fact that our design improvement was found from a global computer optimization, while the design reported in Ref. [30] was found guided by a deliberate, experience-based effort.

Acknowledgements

References

[1] B.N. Brockhouse, Phys. Rev. 98 (1955) 1171.
[2] I. Butterworth, P.A. Egelstaff, H. London, F.J. Webb, Philos. Mag. 2 (1957) 917.
[3] H. Maier-Leibnitz, T. Springer, J. Nucl. Energy A/B 17 (1963) 217.
[4] G. Shirane, S.M. Shapiro, J.M. Tranquada, Neutron Scattering with a Triple Axis Spectrometer, Cambridge University Press, 2002.
[5] See the ILL home page at ⟨www.ill.eu⟩.
[6] See the PSI home page at ⟨www.psi.ch⟩.
[7] See the HZB home page at ⟨www.heltmoltz-berlin.de⟩.
[8] See the NIST home page at ⟨www.nist.gov⟩.
[9] R. Schedler, M. Rotter, M. Löwenhaupt, N.M. Pyka, Appl. Phys. A 74 (2002) S1468.
[10] J.A. Rodriguez, et al., Meas. Sci. Technol. 19 (2008) 034023.
[11] K. Lefmann, K. Nielsen, Neutron News 10 (3) (1999) 42 see also ⟨www.mcstas.org⟩.
[12] S.N. Klausen, et al., Appl. Phys. A 74 (2002) S1508.
[13] L. Udby, et al., Nucl. Instr. and Meth A, this issue, doi:10.1016/j.nima.2010.06.235.
[14] J.K. Hansen, K.S. Hansen, B.P. Christensen, Student Report, University of Roskilde, 2004.
[15] C. Schanzer, P. Böni, U. Filges, T. Hils, Nucl. Instr. and Meth. A 529 (2004) 63.
[16] K.H. Klenø et al., Nucl. Instr. and Meth A, this issue, doi:10.1016/j.nima.2010.06.261.
[17] U. Filges, in preparation.
[18] P. Böni, et al., in: Proceedings of ICANS, 2010.
[19] K. Lefmann, et al., Physica B 283 (2000) 343.
[20] C.R.H. Bahl, P. Andersen, S.N. Klausen, K. Lefmann, Nucl. Instr. and Meth. B. 226 (2004) 667.
[21] See e.g. L.D Landau, E.M. Lifshitz, Course of Theoretical Physics, Statistical Physics, Part 1, vol. 5, Butterworth-Heinemann, 1980.
[22] J. Als-Nielsen, D.F. McMorrow, Elements of Modern X-ray Physics, John Wiley & Sons, 2001.
[23] P. Bentley, et al., these proceedings.
[24] K. Hradil, personal communication, 2010.
[25] C.R.H. Bahl, et al., Nucl. Instr. and Meth. B 246 (2006) 452.
[26] M. Kempa, B. Janusova, J. Saroun, P. Flores, M. Boehm, F. Demmel, J. Kulda, Physica B 385–386 (2006) 1080.
[27] H.R. Rønnow, personal communication, 2010.
[28] J.O. Birk, et al., in preparation.
[29] See the ESS project home page at ⟨www.ess-scandinavia.eu⟩.
[30] M. Janoschek, P. Böni, M. Braden, Nucl. Instr. and Meth. A 613 (2010) 119.